Prediction of Material Removal Rate and Surface Roughness in Electro-Discharge Machining (EDM) Process Based on Neural Network Models

M. Ghoreishi [1*], S. Assarzadeh[2]

1. Assistant Professor of Mechanical Engineering Departmen, K.N. Toosi University of Technology.
2. Postgraduate student of Mechanical Engineering Department, K.N. Toosi University of Technology.

*** P.O. Box: 16765 - 3381, Tehran, Iran**
ghoreishi@kntu.ac.ir

(Received: Oct. 2003, Accepted: Agu. 2005)

Abstract- The complex and stochastic nature of the electro-discharge machining (EDM) process has frustrated numerous attempts of physical modeling. In this paper two supervised neural networks, namely back propagation (BP), and radial basis function (RBF) have been used for modeling the process. The networks have three inputs of current (I), voltage (V) and period of pulses (T) as the independent process variables, and two outputs of material removal rate (MRR) and surface roughness (Ra) as performance characteristics. Experimental data, employed for training the networks and capabilities of the models in predicting the machining behavior have been verified. For comparison, quadratic regression model is also applied to estimate the outputs. The outputs obtained from neural and regression models are compared with experimental results, and the amounts of relative errors have been calculated. Based on these verification errors, it is shown that the radial basis function of neural network is superior in this particular case, and has the average errors of 8.11% and 5.73% in predicting MRR and Ra, respectively. Further analysis of machining process under different input conditions has been investigated and comparison results of modeling with theoretical considerations shows a good agreement, which also proves the feasibility and effectiveness of the adopted approach.

Keywords: Electro-discharge machining (EDM), artificial neural networks (ANNs), Back propagation (BP), Radial basis function (RBF), Process modeling.

1. Introduction

Electro-discharge machining (EDM) is a nontraditional, thermoelectric process, which erodes material from the workpiece by a series of discrete sparks between a workpiece and tool electrode immersed in a liquid dielectric medium. These sparks are generated between two closely spaced electrodes and melt and vaporize tiny amounts of the workpiece, which are then ejected and flushed away by the dielectric [1]. EDM has been used effectively in machining hard, high-strength, and temperature-resistant metals, and since there is no physical contact between the two electrodes, slender and fragile tasks can be machined conveniently, making the process more versatile.

Comprehensive qualitative and quantitative analysis of the material removal mechanism and subsequently the development of model(s) of material removal are not only necessary for a better understanding of the process but are also very useful in parametric optimization, process simulation, operation and process planning, parametric analysis (i.e. understanding the influence of various process parameters on the process performance measures), verification of the experimental results, and improving the process performance by implementing/incorporating some of the theoretical findings [2].

A systematic study of the phenomenon of the electrical discharge in a liquid dielectric has proved to be very difficult due to its complexity. The erosion by an electric discharge involves phenomena such as heat conduction, melting, evaporation, ionization, formation, and collapse of gas bubbles and energy distribution in the discharge channel.

These complicated phenomena coupled with surface irregularities of electrodes, interactions between two successive discharges, and the presence of debris particles make the process too abstruse, there fore complete and accurate physical modeling of the process has not been established yet [3,4].

There are lot of theoretical studies concerned with microscopic metal removal arising from a single spark, the effects being modeled from heat conduction theory [5-8]. Although, these models are based on the physics of process, but due to random distribution of electrical discharges in gap space, and also overlapping effects of two successive sparks, they cannot be developed to multi-spark case, which is the real state of EDM [4].

Recent established models for EDM are mainly based on empirical data or basically data driven models. Ghoreishi and Atkinson [9,10] employed statistical modeling and process optimization for the case of EDM drilling and milling. They have compared the results in vibratory EDM, rotary EDM and a combination of both (vibro-rotary EDM), and concluded that the vibro-rotary electrode compared with the rotary or vibratory cases alone, gives satisfactory results when the most usual combination of requirements, maximum MRR, minimum TWR and constrained surface quality, were considered in an optimization procedure. They have also shown that the best result of employing a vibro-rotary electrode was achieved in the finishing regime when the gap was narrow and there was common difficulty of process instability. In another study, Wang and Tsai [11, 12] proposed semi-empirical models of the material removal rate, surface finish and tool wear on the work and the tool for various materials in EDM, employing dimensional equations based on relevant process parameters for the screening experiments and the dimensional analysis. According to best-fit results from the verification cases, the error analysis showed that the model has reasonable accuracy.

Artificial neural networks (ANNs), as one of the most attractive branches in artificial intelligence, has the potentiality to handle problems such as modeling, estimation, prediction, diagnosis, and adaptive control in complex non-linear systems [13]. The capabilities of ANNs in capturing the mathematical mapping between input variables and output features are of primary significance for modeling of machining processes. The use of neural networks in both EDM and wire-EDM (WEDM) processes has also been reported. Kao and Tarng [14] and Liu and Tarng [15] have employed feed forward neural networks with hyperbolic tangent functions and abductive networks for the classification and on-line recognition of pulse-types. Based on their results, discharge pulses have been identified and then used for controlling the EDM machine. Indurkhya and Rajurkar [16] developed a 9-9-2 size back propagation neural network for orbital EDM modeling. In this case, input parameters were selected as machining depth, tool radius, orbital radius, radial step, vertical step, offset depth, pulse on time, pulse off time and discharge current, and outputs as material removal rate (MRR) and surface roughness (Ra). Having compared the results of neural network model with estimates obtained via multiple regression analysis, they concluded that the network model is more accurate and also less sensitive to noise included in the experimental data. Spedding and Wang [17,18], and Tarng et al. [19] have developed BP neural networks for modeling of WEDM. Experimental results have shown that the cutting performance of WEDM can be greatly enhanced using the neural model.

The objective of this paper is to establish neural network models for predicting material removal rate (MRR) and surface roughness (Ra). More specifically, two different types of neural networks, back propagation (BP) and radial basis function (RBF) are used to construct the process models. Effective parameters influencing process outputs and their levels for training experiments were selected through preliminary tests carried out on an EDM machine. Networks trained by the same experimental data are then verified by some experiments different from those used in training phase, and the best model was selected based on the criterion of having the least average values of verification errors. In addition, quadratic regression model was also incorporated in this research to compare the accuracy of neural models with this common statistical model.

The capabilities of the best model in predicting process outputs under varying input machining conditions were also analyzed, and finally, the paper concludes with a summary of this study.

2. Overview of Neural Networks

A neural network is a massive parallel system comprised of highly interconnected, interacting processing elements, or nodes. Neural networks process through the interactions of a large number of simple processing elements or nodes, also known as neurons. Knowledge is not stored within individual processing elements, rather represented by the strengths of the connections between elements. Each piece of knowledge is a pattern of activity spread among many processing elements, and each processing element can be involved in the partial representation of many pieces of information.

In recent years, neural networks have become a very useful tool in the modeling of complicated systems [13] because it has an excellent ability learn and to generalize (interpolate) the complicated relationships between input and output variables. Also, the ANNs behave as model free estimators, i.e., they can capture and model complex input-output relations without the help of a mathematical model [20]. In other words, training neural networks for example eliminates the need for explicit mathematical modeling or similar system analysis. This property of ANNs is extremely useful in a situation where it is hard to derive a mathematical model. As a result, neural networks can provide an effective solution to solve problems that are intractable or cumbersome with mathematical approaches.

3. Artificial Neural Network Models of EDM Process

In this research back-propagation (BP) and radial basis function (RBF) neural networks have been used for modeling the process due to their universal approximation capabilities [21]. The first ANN is very popular, especially in the area of on-line monitoring and manufacturing modeling, as its design, structure and operation are relatively simple. The radial basis network has some additional advantages such as rapid learning and less error. In particular, most RBFNs involve fixed basis functions with linearly unknown parameters in the output layer. In contrast, multi-layer BP ANNs comprise adjustable basis functions, which results in nonlinearly unknown parameters. It is commonly known that linear parameters in RBFN makes the use of least squares error based updating schemes possible that have faster convergence than the gradient-descent methods in multi-layer BP ANN. On the other hand, in practice, the number of parameters in RBFN starts becoming unmanageably large only when the number of input features increases beyond 10 or 20, which is not the case in our study. Hence, the use of RBFN was practically possible in this research.

In this paper, MATLAB Neural Network Toolbox “NNET” was used as a platform to create the networks.

3.1. Back-Propagation (BP) Neural Network

The back-propagation network (Fig. 1) is composed of many interconnected neurons or processing elements (PE) operating in parallel and are often grouped in different layers.

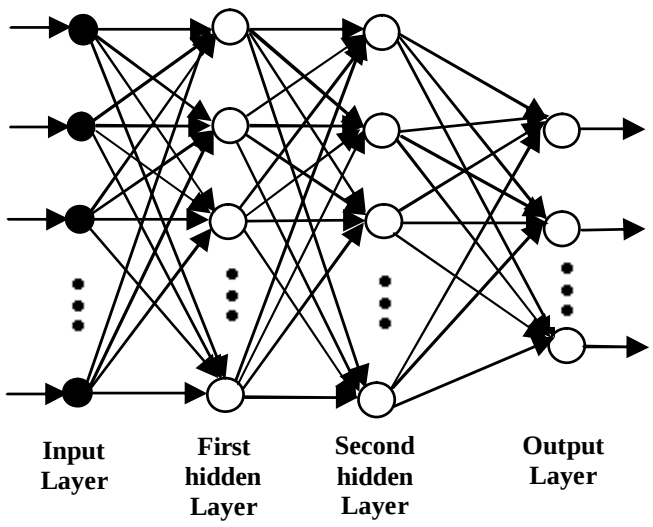

Fig. 1 Back-propagation neural network with two hidden layers.

As shown in Fig. 2, each artificial neuron evaluates the inputs and determines the strength of each through its weighing factor. In the artificial neuron, the weighed inputs are summed to determine an activation level. That is,

$$net_j^k = \sum_i w_{ji}^k o_i^{k-1} \quad (1)$$

where net_j^k is the summation of all the inputs of the jth neuron in the kth layer, w_{ji}^k is the weight from the ith neuron to the jth neuron

and o_i^{k-1} is the output of the ith neuron in the (k-1)th layer.

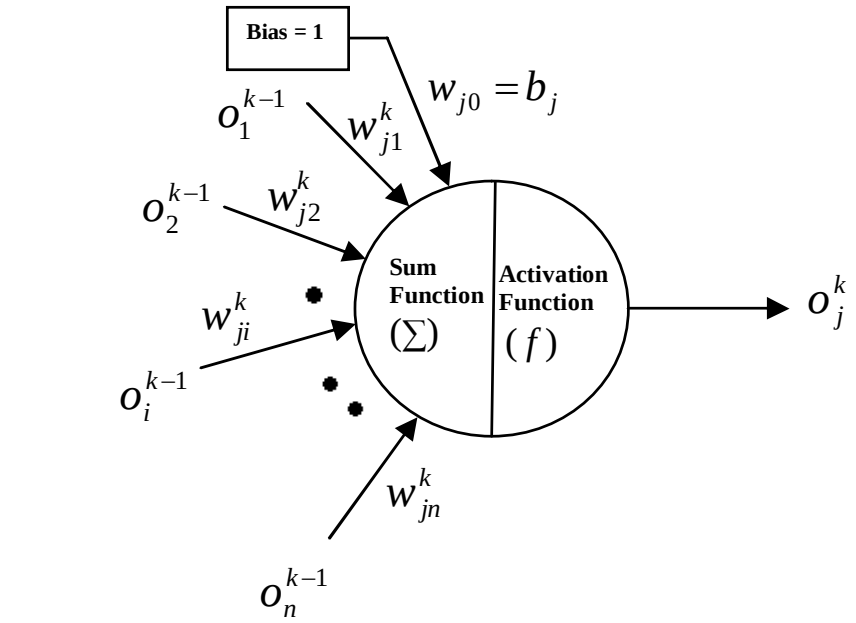

Fig. 2 Architecture of an individual PE for BP network.

The output of the neuron is then transmitted along the weighed outgoing connections to serve as an input to subsequent neurons. In the present study, a hyperbolic tangent function $f(net_j^k)$ with a bias b_j is used as an activation function of hidden and output neurons. Therefore, output of the jth neuron o_j^k for the kth layer can be expressed as:

$$o_j^k = f(net_j^k) = \frac{e^{(net_j^k + b_j)} - e^{-(net_j^k + b_j)}}{e^{(net_j^k + b_j)} + e^{-(net_j^k + b_j)}} \quad (2)$$

Before practical application, the network has to be trained. To properly modify the connection weights, an error-correcting technique, often called as back-propagation learning algorithm or generalized delta rule [13] is employed. Generally, this technique involves two phases through different layers of the network. The first is the forward phase, which occurs when an input vector is presented and propagated forward through the network to compute an output for each neuron. During the forward phase, synaptic weights are all fixed. The error obtained when a training pair (pattern-'p') consisting both input and output given to the input layer of the network, is expressed by the following equation:

$$E_p = \frac{1}{2}\sum_j (T_{pj} - O_{pj})^2 \quad (3)$$

where, T_{pj} is the jth component of the desired output vector, and O_{pj} is the calculated output of jth neuron in the output layer. The overall error of all the patterns in the training set is defined as mean square error (MSE) and is given by:

$$E = \frac{1}{p}\sum_{p=1}^{n} E_p \quad (4)$$

where n is the number of input-output patterns in the training set.

The second is the backward phase which is an iterative error reduction performed in the backward direction from the output layer to the input layer. In order to minimize the error, E, as rapidly as possible, the gradient descent method, adding a momentum term is used.

Hence, the new incremental change of weight $\Delta w_{ji}^k(m+1)$ can be:

$$\Delta w_{ji}^k(m+1) = -\eta \frac{\partial E}{\partial w_{ji}^k} + \alpha \Delta w_{ji}^k(m) \quad (5)$$

where η is a constant real number between 0.1 and 1, called learning rate, α is the momentum parameter usually set to a number between 0 and 1, and m is the index of iteration. Therefore, the recursive formula for updating the connection weights become:

$$w_{ji}^k(m+1) = w_{ji}^k(m) + \Delta w_{ji}^k(m+1) \quad (6)$$

These corrections can be made incrementally (after each pattern presentation) or in batch mode. In the latter case, the weights are updated only after the entire training pattern set has been applied to the network. With this method, the order in which the patterns are presented to the network does not influence the training. This is because of the fact that adaptation is done only at the end of each epoch. And thus, we have chosen this way of updating the connection weights.

3.2. Radial Basis Function (RBF) Neural Network

The construction of a radial basis function (RBF) neural network in its most basic form involves three entirely different layers. A typical RBFN with N input and M output is shown in Fig. 3. The input layer is made up of source nodes (sensory units). The second layer is a single hidden layer of high enough dimension, which serves a different purpose in a feed-forward network. The output layer supplies the response of the network to the activation patterns applied to the input layer.

The input units are fully connected though unit-weighed links to the hidden neurons, and the hidden neurons are fully connected by weighed links to the output neurons. Each hidden neuron receives input vector $\boldsymbol{X}$ and compares it with the position of the center of Gaussian activation function with regard to distance. Finally, the output of the jth-hidden neuron can be written as:

$$A_j = \exp\left(-\frac{\left\|\mathbf{X}_i - \mathbf{C}_j\right\|^2}{S^2}\right) \quad (7)$$

where, $\boldsymbol{X}_i$ is an N-dimensional input vector, $\boldsymbol{C}_j$ is the vector representing the position of the center of the jth hidden neuron in the input space, and S is the standard deviation or spread factor of Gaussian activation function. The structure of a radial basis neuron in the hidden layer can be seen in Fig. 4.

Output neurons have linear activation functions, and form a weighted linear combination of the outputs from the hidden layer:

$$Y_k = \sum_{j=1}^{H} w_{kj} A_j \quad (8)$$

where, Y_k is the output of neuron k, H is the number of hidden neurons, and w_{kj} is the weight value from the jth hidden neuron to the kth output neuron.

Basically, the RBFN has the properties of rapid learning, easy convergence, and less error, Generally possess following characteristics:

1- It may require more neurons than the standard feed-forward BP networks;

2- It can be designed in a fraction of the time that it takes to train the BP network;

3- It has excellent ability of representing nonlinear functions.

RBFN is being used for an increasing number of applications, proportioning a very helpful modeling tool.

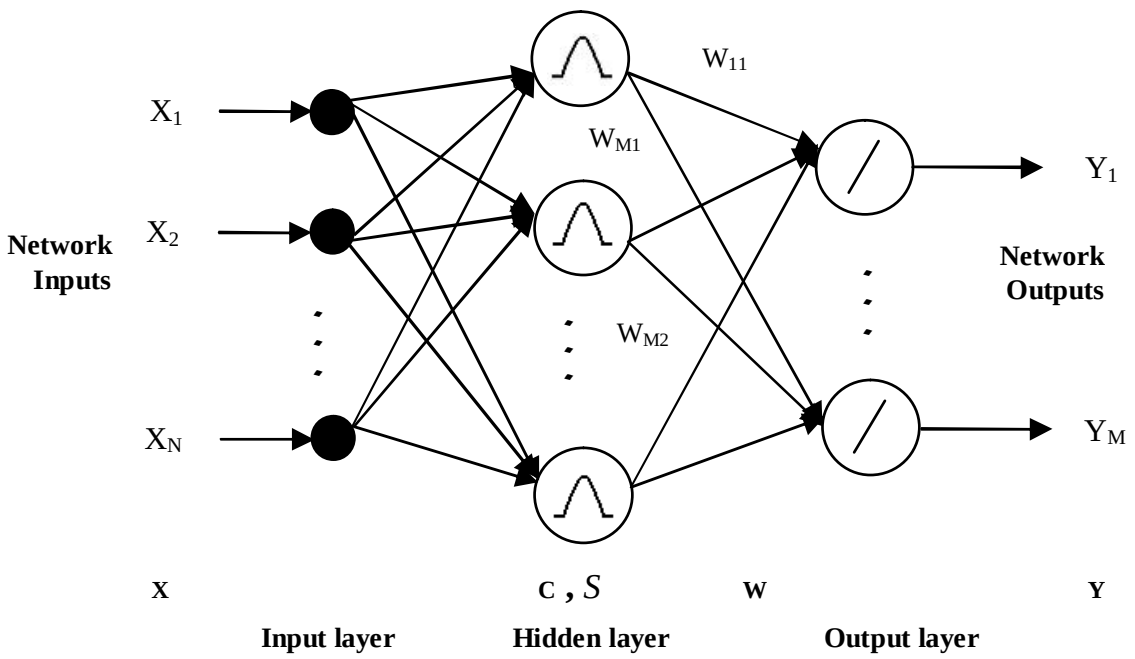

Fig. 3 Radial basis function neural network.

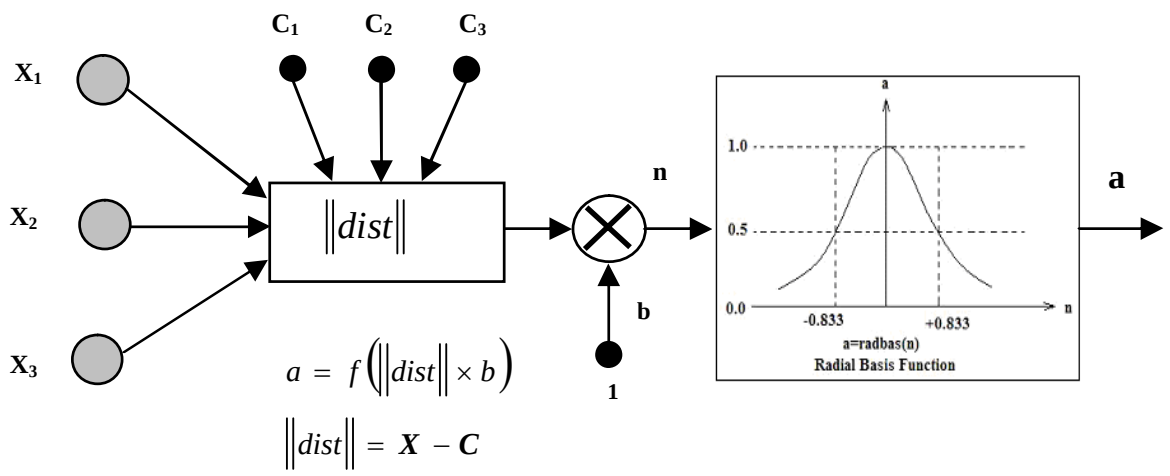

Fig. 4 Radial basis neuron.

4. Experimental Details

In order to obtain different machining process parameters and output features for training and testing of neural networks, a series of experiments was performed on a Pishtazan electro-discharge machine (Model SP120A) equipped with an iso-frequency pulse generator.

At first, some preliminary tests were carried out to determine the stable domain of the machine parameters and also the different ranges of process variables. Based on preliminary tests results and working characteristics of the EDM machine, discharge current (I), period of pulses (T), and source voltage (V) were chosen as independent input parameters. During these experiments, by altering the values of the input parameters in different levels, stable states of the machining conditions was also specified. Accordingly, the experiments were conducted with six levels of discharge current, four levels of period of pulses, and four levels of source voltage. Table 1 shows the input process variables and their levels in the experiments.

Table 1 Pertinent process parameters and their levels for machining experiments.

Process parameters	perating conditions
Discharge current I (A)	2, 5, 8, 11, 14, 17
Period of pulses T (μs)	50, 100, 200, 500
Source voltage V (v)	35, 50, 60, 70

Throughout the experiments, SPK 2080 steel and commercial copper were used as workpiece and tool electrode materials. Workpieces were heat treated up to 58 RC to establish real and practical situations in all tests. Also, the dielectric fluid used was kerosene. Particular attention was paid to ensure that operating conditions permitted effective flushing of machining debris from the working region. Thus, the experiments were conducted in the planing process mode in which the bottom surface of the electrode is flat and parallel to the workpiece surface. Also, the diameter of cylindrical electrode was equal to the diameter of the round bar workpiece and was chosen to be 12 mm.

The total data obtained from machining experiments (6*4*4) is 96 which forms the neural networks' training and testing sets. To achieve validity and accuracy, each test was repeated three times. Material removal rate (MRR) and surface roughness (Ra) were considered as performance characteristics or process outputs, since the performance of any machining process is being evaluated in terms of these two measures. Then, the mean values of the three response measurements (MRR and Ra) were used as output at each set of parameters. The machining time considered for each test was dependent on the discharge current and much time was allocated to the tests with lower current.

The material removal rate (MRR) was estimated by weighing the workpiece on a digital single pan balance before and after the experiments and was reported in gr/hr unit. The surface roughness (Ra) was measured by means of a Surtronic 3+ with Ra value in microns at a cut-off length of 0.8 mm.

The results of the experiments show that the training data cover the wide variety of possible ranges, i.e., in our case, three main groups of finishing ($Ra \leq 2$), semi-finishing ($2 \prec Ra \leq 4$), and roughing ($Ra \succ 4$) are involved.

5. Modeling of EDM Process Using Neural Networks

Modeling of EDM process with BP and RBF neural networks is composed of two stages: training and testing of the networks with experimental machining data. The training data consisted of values for current (I), period of pulses (T), and source voltage (V), and the corresponding material removal rate (MRR) and surface roughness (Ra). total 96 such data sets were used, of which 82 were selected randomly and used for training purposes whilst the remaining 14 data sets were presented to the trained networks as new application data for verification (testing) purposes. Thus, the networks were evaluated using data that had not been used for training.

Before the ANN could be trained and the mapping learnt, it is important to process the experimental data into patterns. Training/Testing pattern vectors are formed, each formed with an input condition vector, P_i

$$P_i = \begin{bmatrix} \text{Current (I)} \\ \text{Period of pulses (T)} \\ \text{Voltage (V)} \end{bmatrix}$$

and the corresponding target vector, T_i

$$T_i = \begin{bmatrix} \text{Material removal rate (MRR)} \\ \text{Surface roughness (Ra)} \end{bmatrix}$$

Mapping each term to a value between -1 and 1 using the following linear mapping formula:

$$N = \frac{(R - R_{\min}) * (N_{\max} - N_{\min})}{(R_{\max} - R_{\min})} + N_{\min} \qquad (9)$$

where, N : normalized value of the real variable; $N_{\min} = -1$ and $N_{\max} = 1$: minimum and maximum values of normalization, respectively; R : real value of the variable; $R_{\min}$ and $R_{\max}$: minimum and maximum values of the real variable, respectively.

These normalized data was used as the inputs (machining conditions) and outputs (performance characteristics) to train the ANN. In other words, the network has three inputs of current (I), period of pulses (T) and source voltage (V) and two outputs of material removal rate (MRR) and surface roughness (Ra). Fig. 5 shows the general network topology for modeling the process.

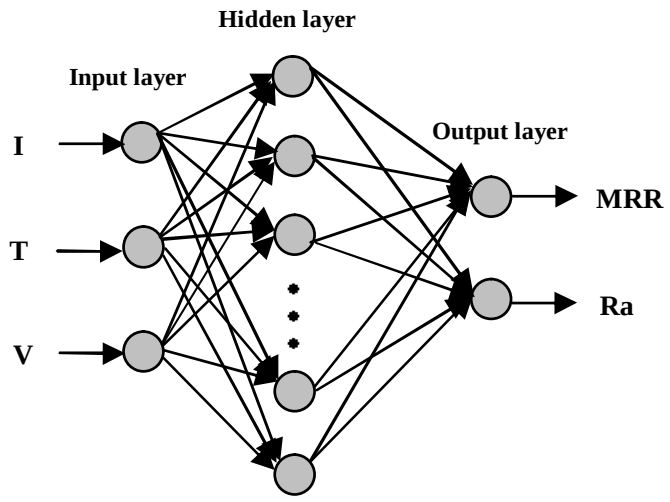

Fig. 5 General ANN topology.

In what follows, the use of two neural networks will be discussed and the results are presented. Then, the best model is picked based on the accuracy of predicting the machining behavior in the verification stage. The results of regression model will also be illustrated for the sake of comparison. Finally, the effects of input parameters on process outputs are analyzed using the best model.

5.1. BP Neural Network Model

The size of hidden layer(s) is one of the most important considerations when solving actual problems using multi-layer feed-forward network. However, it has been shown that BP neural network with one hidden layer can uniformly approximate any continuous function to any desired degree of accuracy given an adequate number of neurons in the hidden layer and the correct interconnection weights [22]. Therefore, one hidden layer was adopted for the BP model. to determin the number of neurons in the hidden layer, a procedure of trail and error approach needs to be done. As such, attempts have been made to study the network performance with a different number of hidden neurons. Hence, a number of candidate networks are constructed, each of trained separately, and the “best” network were selected based on the accuracy of the predictions in the testing phase. It should be noted that if the number of hidden neurons is too large, the ANN might be over-trained giving spurious values in the testing phase. If too few neurons are selected, the function mapping might not be accomplished due to under-training. Table 2 shows 14 experimental data sets, used for verifying or testing network capabilities in modeling the process.

Table 2 Machining conditions for verification experiments.

Test No.	I (A)	T (µs)	V (v)	MRR (gr/hr)	Ra (µm)
1	5	500	35	0.7	3.05
2	5	100	50	3.54	3.28
3	8	50	70	5.45	4.27
4	8	200	50	6.39	4.52
5	8	50	60	7.72	4.85
6	11	500	70	5.97	4.92
7	11	100	70	10.64	5.25
8	11	200	60	11.83	5.45
9	11	200	35	21.01	6.9
10	14	500	50	9.52	5.12
11	14	50	50	15.3	6.1
12	14	100	60	18.64	7.3
13	17	50	35	24.27	7.2
14	17	100	35	27.51	7.32

Therefore, the general network structure is supposed to be 3-n-2, which implies 3 neurons in the input layer, n neurons in the hidden layer, and 2 neurons in the output layer. Then, by varying the number of hidden neurons, different network configurations are trained, and their performances are checked. The results are shown in Table 3.

Table 3 The effects of different number of hidden neurons on the BP network performance.

No. of hidden neurons	Epoch	Average error in MRR (%)	Average error in Ra (%)	Total average error (%)
4	16824	12.31	7.46	9.88
5	4970	16.38	6.87	11.62
6	1773	10.19	7.47	8.83
7	984	19.72	10.05	14.89
8	844	30.84	6.49	18.67

For training problem, equal learning rate and momentum constant of $\eta = \alpha = 0.9$ were used. Also, error stopping criterion was set at E=0.01, which means training epochs continued until the mean square error fell beneath this value. Both the required iteration numbers and mapping performances were examined for these networks. As the error criterion for all networks was the same, their performances are comparable. As a result, from Table 3, the best network structure of BP model is picked to have 6 neurons in the hidden layer with the average verification errors of 10.19% and 7.47% in predicting MRR and Ra, respectively. Thus, it has a total average error of 8.83% over the 14 experimental verification data sets. Table 4 shows the comparison of experimental and predicted values for MRR and Ra in verification cases.

Fig. 6 illustrates the convergence of the output error (mean square error) with the number of iterations (epochs) during training of the chosen 3-6-2 BP network. After 1773 epochs, the MSE between the desired and actual outputs becomes less than 0.01. At the beginning of the training, the output from the network is far from the target value. However, the output slowly and geadually converges to the target value with more epochs and the network learns the input/output relation of the training samples.

5.2. RBF Neural Network Model

Spread factor (S) value of Gaussian activation functions in the hidden layer is the parameter that should be determined by trail and error when using MATLAB neural network toolbox for designing RBF networks. It has to be larger than the distance between adjacent input vectors, so as to get good generalization, but smaller than the distance across the whole input space [23]. Based on this, and considering that all the training data (as explained in section 5) has been spanned in the range of -1 and +1, the upper and lower limits of the spread factor will become:

$$min(S) = \sqrt{((-1+0.6)^2 + (-1+1)^2 + (-1+1)^2)} = 0.4$$

$$max(S) = \sqrt{((-1-1)^2 + (-1-1)^2 + (-1-1)^2)} = 3.46$$

where, [-1,-1,-1] is the left-most or the first training input vector, [-0.6,-1,-1] is the second or adjacent input vector, and [1,1,1] is the right-most or the last input vector available in the scaled training data set. Therefore, in order to have a network model with good generalization capabilities, the spread factor should be selected between 0.4 and 3.46. For training the RBF network, at first, a guess is made for the value of spread factor in the obtained interval. Also, the number of radial basis neurons is originally set as 1. At each iteration, the input vector that results in lowering the most network training error, is used to create a radial basis neuron. Then, the error of the new network is checked, and if it is low enough, the training stopped. Otherwise, the next neuron is added. This procedure is repeated until the error goal is achieved, or the maximum number of neurons is reached. In the present case, it was found by trail and error that 22 hidden neurons with the spread factor of 2, can give a model, which has the best performance in the verification stage. Table 5 shows the effect of the number of hidden neurons on the RBF network performance. It is clear that althoughly adding hidden neurons more than 22 makes the training error (MSE) smaller, however deteriorates network's generalization capabilities with the increase of average verification errors instead of decreasing.

Therefore, the optimum number of radial basis neurons is 22. The selected network has the average errors of 8.11% and 5.73% in response to the 14 input verification experiments (Table 2) for MRR and Ra respectively. Table 6 lists output values predicted by the RBF neural model and experimental ones in verification (testing) phase.

Table 4 Comparison of MRR and Ra measured and predicted by the BP neural network model.

Test No.	MRR (gr/hr)		Ra (μm)		Error (%)	
	Experimental	BP model	Experimental	BP model	Error in MRR	Error in Ra
1	0.7	0.76	3.05	2.48	8.57	18.69
2	3.54	3.13	3.28	3.40	11.58	3.66
3	5.45	6.49	4.27	4.24	19.08	0.70
4	6.39	5.95	4.52	4.38	6.89	3.1
5	7.72	7.02	4.85	4.26	9.07	12.16
6	5.97	3.42	4.92	4.80	42.71	2.44
7	10.64	12.16	5.25	5.72	14.29	8.95
8	11.83	11.95	5.45	5.82	1.01	6.79
9	21.01	19.87	6.9	6.30	5.43	8.70
10	9.52	8.83	5.12	6.26	7.25	22.27
11	15.3	16.99	6.1	6.58	11.05	7.87
12	18.64	18.74	7.3	6.90	0.54	5.48
13	24.27	24.59	7.2	7.32	1.32	1.67
14	27.51	26.44	7.32	7.47	3.89	2.05

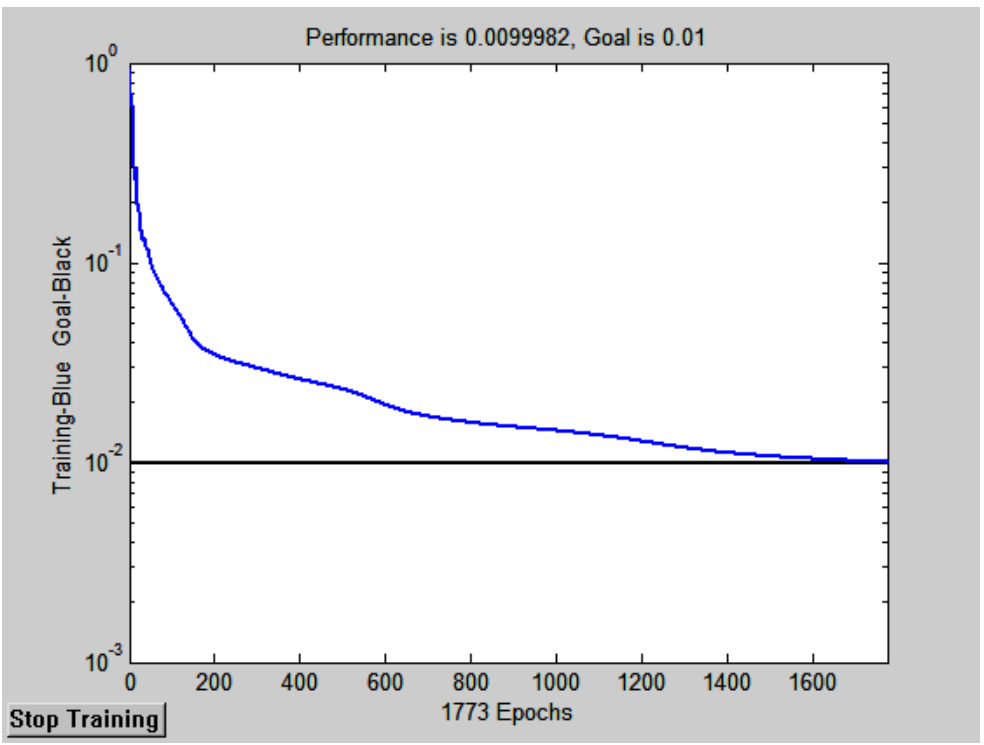

Fig. 6 Learning behavior of the BP neural network model.

Table 5 The effects of different number of hidden neurons on the RBF network performance (S=2).

No. of hidden neurons	Training error (MSE)	Average error in predicting MRR (%)	Average error in predicting Ra (%)	Total average error (%)
16	0.0151	16.87	7.3	12.09
18	0.014	9.66	6.77	8.22
20	0.0131	10.13	6.02	8.08
22	0.012	8.11	5.73	6.92
24	0.0115	11.32	6.71	9.02
26	0.0113	11.72	7.7	9.71
28	0.0107	12.02	8.48	10.25

6. Selection of the Best Model

The simplest approach to the comparison of different networks is to evaluate the error function using data which is independent of that used for training [24]. Hence, the selection of the corresponding “best network” is carried out based on the accuracy of predicting the process outputs in verification stage.

From Tables 3 and 5, it is concluded that RBFN model with the total average error of 6.92% in comparison with 8.83% for BP model, has superior performance, and therefore is picked as the best model. Figures 7 and 8 illustrate the experimental and predicted MRR and Ra by BP and RBF neural networks in verification stages, respectively.

As a further step to study the capabilities of each network in fitting all points in the input space, a linear regression between the network outputs and the corresponding target (empirical) values was performed. In this case, the entire data set (training and verification) was put through the trained networks, and regression analysis was conducted.

The results are presented separately for the two output parameters (see Figures 9, 10). The networks have mapped each of the two outputs very well. The correlation coefficients (R) are also given as a criterion of comparison. The amounts of R are 0.988 and 0.98 for BP model, and 0.991 and 0.988 for RBF model in simulating MRR and Ra, respectively. Again, it is inferred that RBF network still has better capabilities in fitting all the data in the input space, and therefore can be used to acquire a function that maps input parameters to the desired process outputs in a wide range of machining conditions.

Table 6 Comparison of MRR and Ra measured and predicted by the RBF neural network model.

Test No.	MRR (gr/hr)		Ra (μm)		Error (%)	
	Experimental	RBF model	Experimental	RBF model	Error in MRR	Error in Ra
1	0.7	0.58	3.05	3.14	16.69	2.89
2	3.54	2.51	3.28	3.55	29.19	8.29
3	5.45	6.51	4.27	4.19	19.52	1.89
4	6.39	6.47	4.52	4.47	1.27	1.05
5	7.72	7.74	4.85	4.58	0.28	5.59
6	5.97	5.40	4.92	5.23	9.60	6.32
7	10.64	11.45	5.25	5.85	7.59	11.47
8	11.83	12.90	5.45	5.75	9.01	5.55
9	21.01	19.69	6.9	6.79	6.27	1.59
10	9.52	9.80	5.12	5.34	2.91	4.34
11	15.3	16.94	6.1	6.27	10.71	2.77
12	18.64	18.61	7.3	7.03	0.14	3.74
13	24.27	24.19	7.2	5.93	0.32	17.60
14	27.51	27.51	7.32	6.80	0.01	7.07

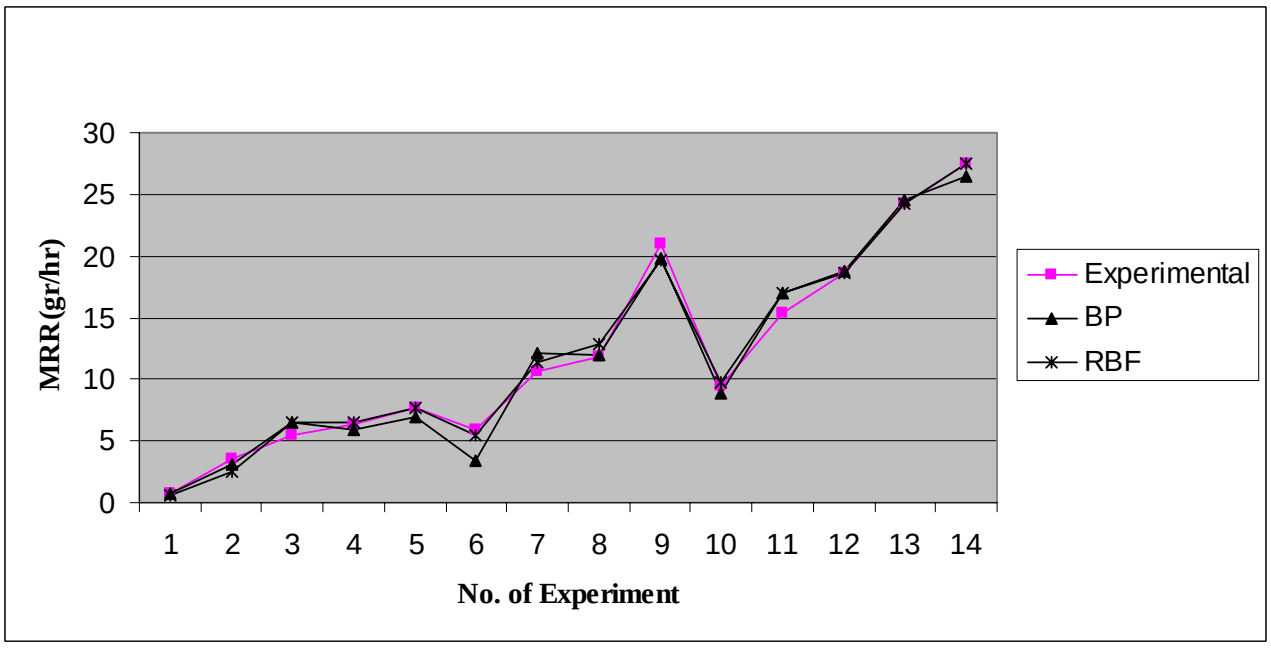

Fig. 7 The comparison of MRR between verification and experimental results.

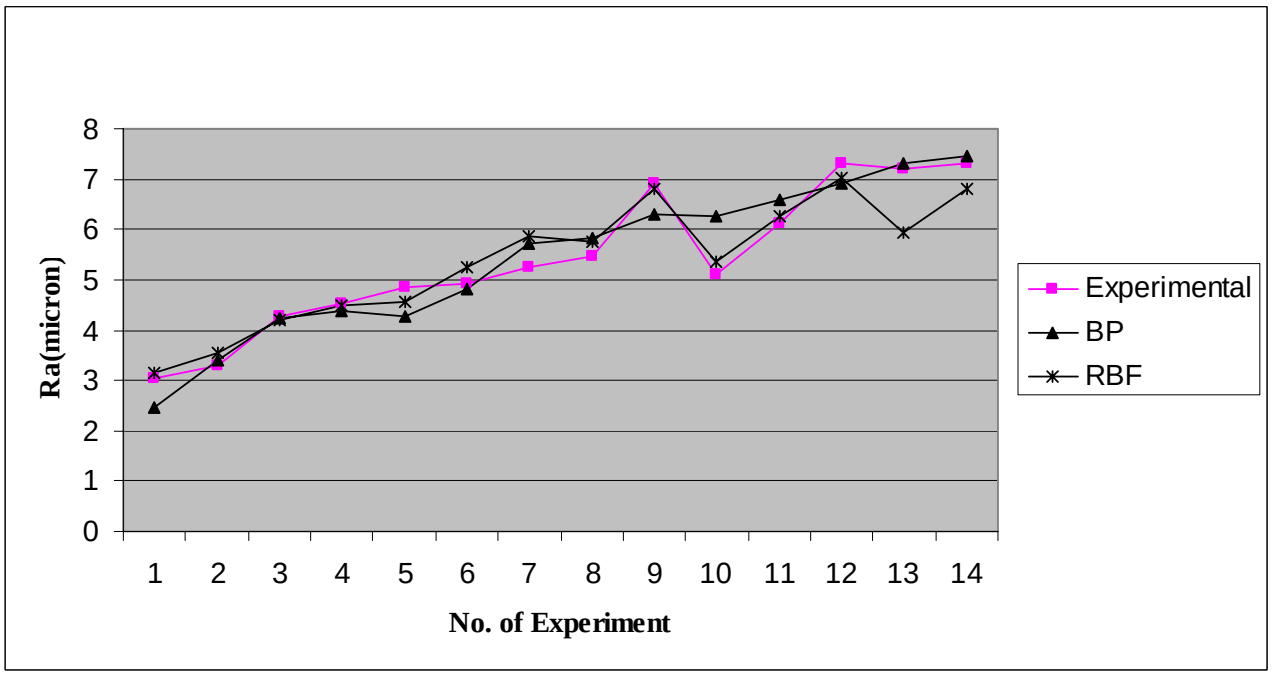

Fig. 8 The comparison of Ra between verification and experimental results.

(a) (b)

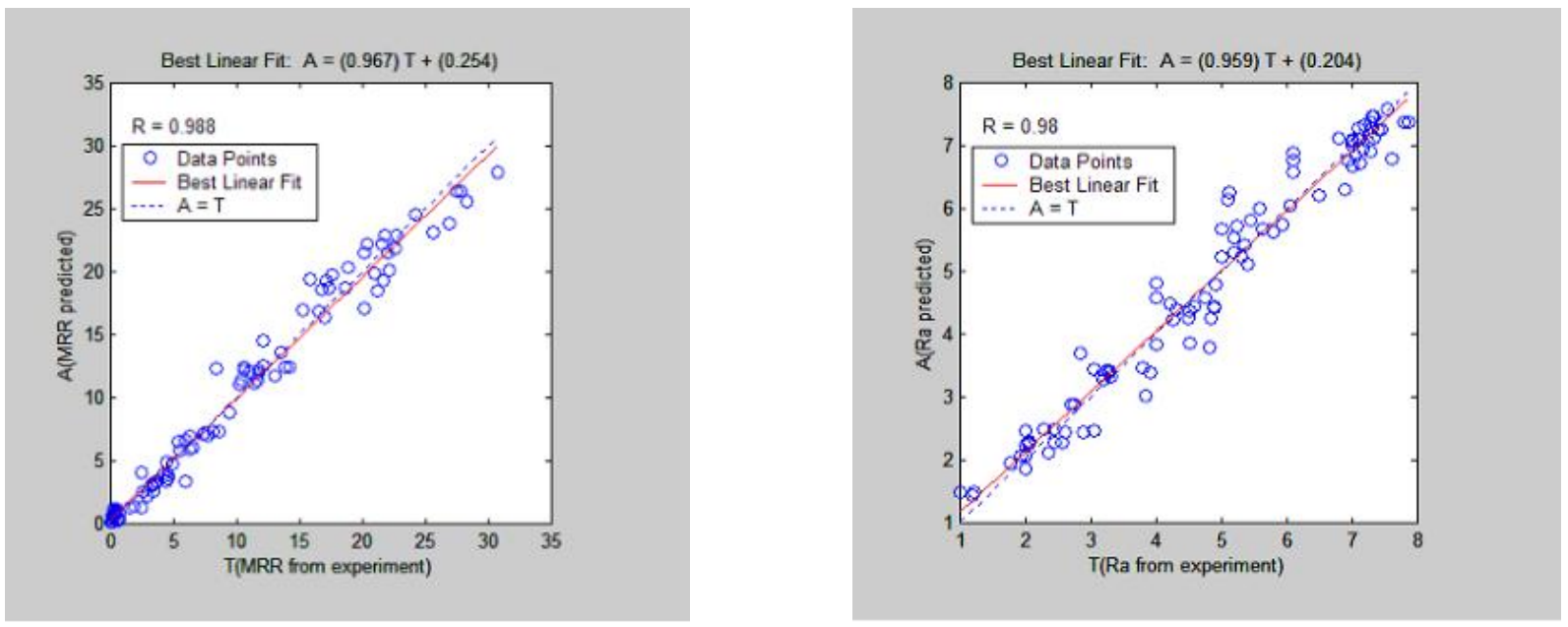

Fig. 9 Linear regression analysis between BP network outputs and experimental values: (a) MRR and (b) Ra.

(a) (b)

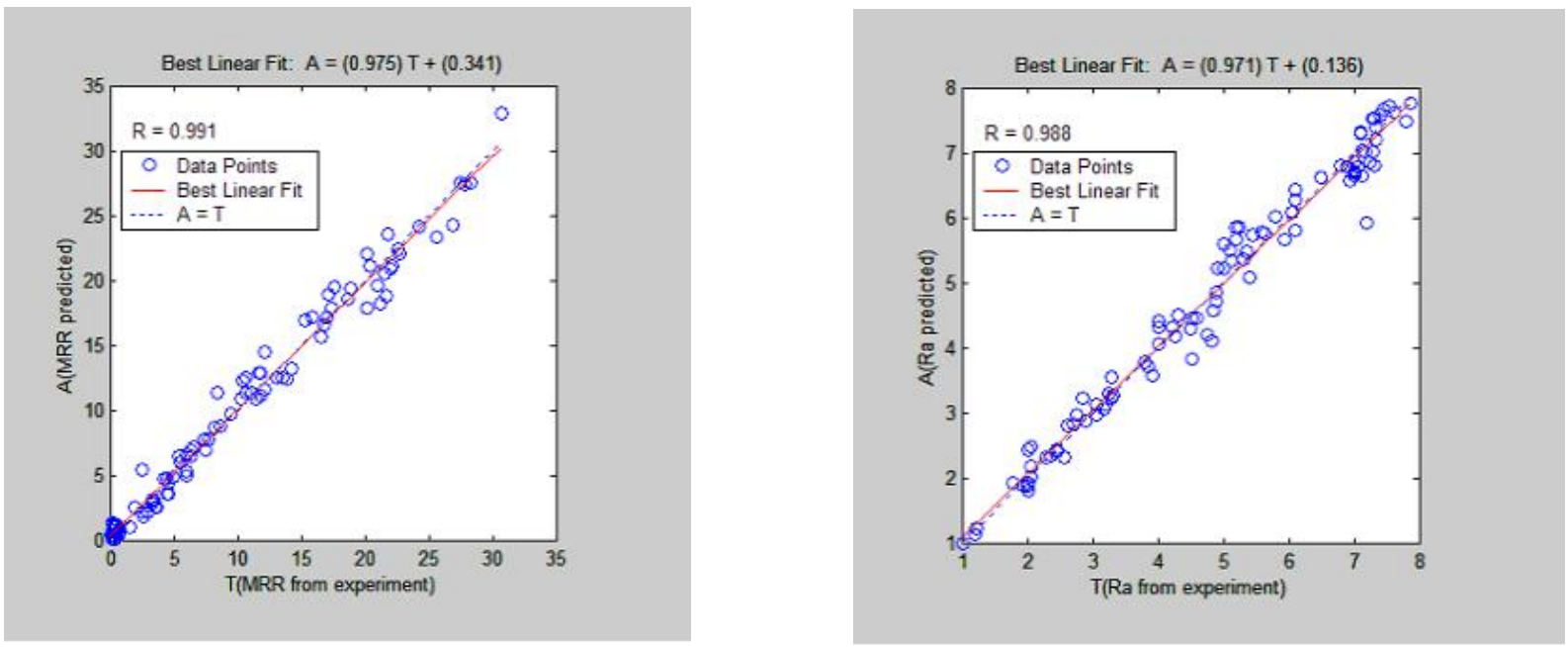

Fig. 10 Linear regression analysis between RBF network outputs and experimental values: (a) MRR and (b) Ra.

7. Quadratic Regression Model of EDM Process

To compare the accuracy of neural networks with common statistical modeling techniques, quadratic regression model has also been developed. This mathematical model includes linear, squared and interaction terms of process variables for each response (process output). By this mean, any non-linearity or curvature in the response would be considered. In scalar notion, a fitted second order model is [25]:

$$\eta = \beta_0 + \sum_{j=1}^{k} \beta_j x_j + \sum_{j=1}^{k} \beta_{jj} x_j^2 + \sum\sum_{i<j} \beta_{ij} x_i x_j \qquad (10)$$

where k is the number of independent variables. In this case, k=3. The coefficient β_0 represents the response at the center of the experiment when all of the variables are 0. The β_j, β_{jj}, and β_{ij} represent the coefficients of linear, quadratic and linear-by-linear interaction effects of the variables respectively. The regression coefficients were computed according to the least squares procedure. More details can be found in [26]. In our case, for each process output (MRR and Ra) equation (10) will become:

$$MRR = a_0 + a_1 I + a_2 T + a_3 V + a_4 IT + a_5 IV + a_6 TV + a_7 I^2 + a_8 T^2 + a_9 V^2$$

$$Ra = b_0 + b_1 I + b_2 T + b_3 V + b_4 IT + b_5 IV + b_6 TV + b_7 I^2 + b_8 T^2 + b_9 V^2$$

where the a_i's and b_i's coefficients are as follow:

$$a_0 = 7.5516, a_1 = 2.1578, a_2 = 0.037181, a_3 = -0.56482,$$
$$a_4 = -0.00082, a_5 = -0.01963, a_6 = -0.00014, a_7 = 0.029058,$$
$$a_8 = -5.73E-5, a_9 = 0.006115$$
$$b_0 = 4.5591, b_1 = 0.37216, b_2 = 0.005597, b_3 = -0.12664,$$
$$b_4 = 0.000115, b_5 = 0.000813, b_6 = -3.15E-5, b_7 = -0.00442,$$
$$b_8 = -1.2E-5, b_9 = 0.001144$$

The results obtained from the above equations for 14 input machining conditions shown in Table 2 indicate that ANNs are giving more accurate outputs in comparison to experimental ones. Table 7 shows the final modeling results achieved via BP and RBF neural networks as well as quadratic model as a ready reference.

It is shown that the amount of total average errors of BP and RBF models are lower than that of regression model. Therefore, this confirms the suitability and also superiority of the adopted neural networks with respect to statistical methods in the present case.

Table 7 Final modeling results from neural and regression methods.

Model	Average error in prediction of MRR (%)	Average error in prediction of Ra (%)	Total average error (%)
BP network	10.19	7.47	8.83
RBF network	8.11	5.73	6.92
Quadratic regression	40.24	14.35	27.30

8. Effects of the Input Parameters on the Output Features

In the following, the effects of the machining parameters on the process outputs will be discussed one by one based on the developed RBF neural network (the best model). To separate the effect caused by each machining parameter, the other input variables are set to a constant value in the allowable working spaces when one of the machining parameters is varied and analyzed.

8.1. Effect of discharge current

The effect of current on EDM characteristics (MRR and Ra) is shown in Figures 11 and 12, respectively, under different pulse periods, and 55v source voltage.

At all values of pulse periods, both the material removal rate and surface roughness increase steadily with the increase of current. This was expected, because MRR and Ra depend on the spark energy, which is directly proportional to the intensity of current. Therefore, increasing current results in greater discharge of energy, rising material removal rate and leading to poor surface quality.

8.2. Effect of pulse period

The effect of pulse period (pulse-on time + pulse-off time) on MRR and Ra is depicted in Figures 13 and 14, respectively, for various source voltage settings at a constant current of 9A. It is showed that the values of material removal rate and surface roughness are highest with the pulse period of about 150 μsec. However, with longer pulse period, MRR and Ra decrease.

This can be explained from the fact that although spark energy increases with increasing pulse-on time, but too long pulse period causes unfavorable heat losses in the gap space, which does not contribute to the material removal. Therefore, keeping other factors constant, there is an optimum value of pulse period in which the highest MRR occurs.

8. 3. Effect of source voltage

The effect of source voltage on MRR and Ra is illustrated in Figures 15 and 16, respectively, for different current values at a constant pulse period of 250 μsec. There are slight changes in MRR and Ra with respect to source voltage variations. In other words, the source voltage in the working domain considered in experiments has not influenced material removal and surface roughness considerably.

9. Conclusions and Summary

In this paper, two supervised neural networks have been used for the successful EDM process. An effort was made to include as many different machining conditions as possible that influence the process. Based on the test results of each network with some data set, different from those used in the training phase, it was shown that RBF neural model has superior performance than BP network as well as regression model, and can predict process outputs in a wide range of machining conditions with reasonable accuracy.

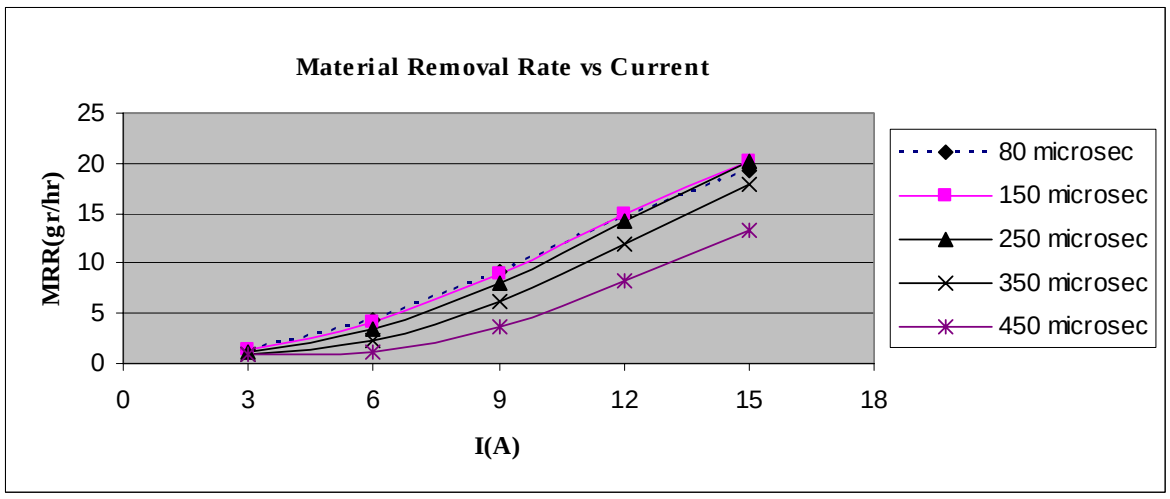

Fig. 11 Effect of current on material removal rate.

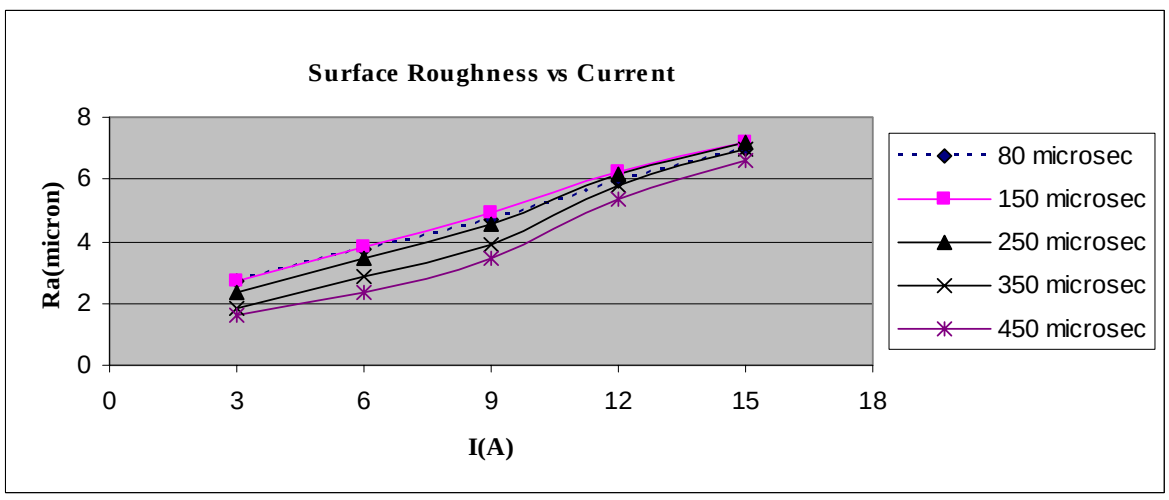

Fig. 12 Effect of current on workpiece surface roughness.

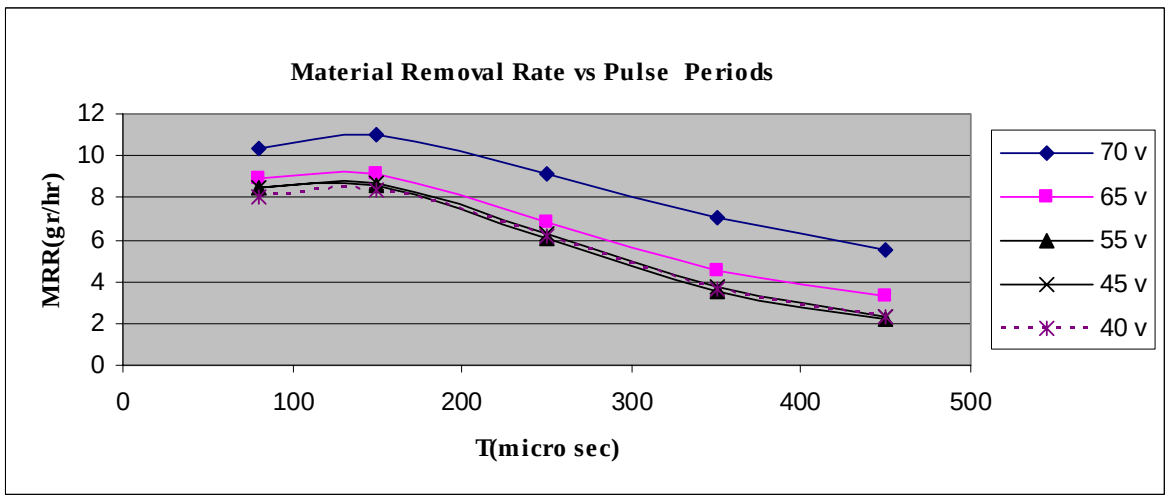

Fig. 13 Effect of pulse period on material removal rate.

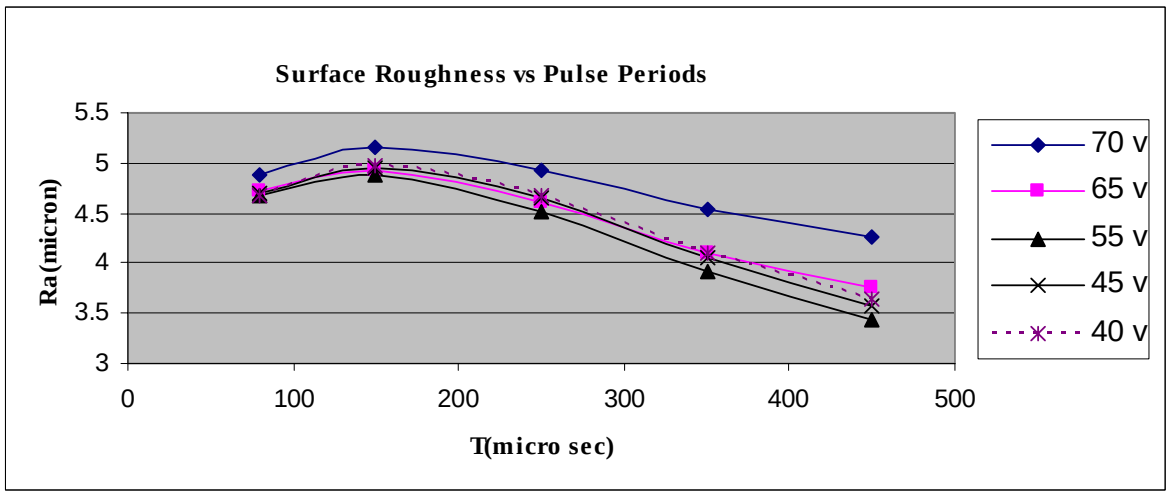

Fig. 14 Effect of pulse period on workpiece surface roughness.

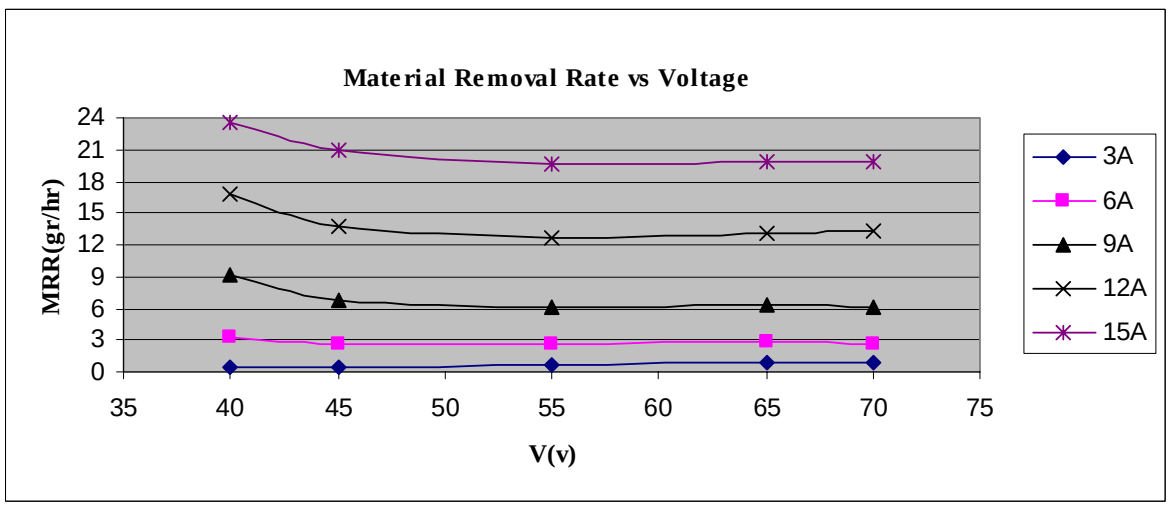

Fig. 15 Effect of source voltage on material removal rate.

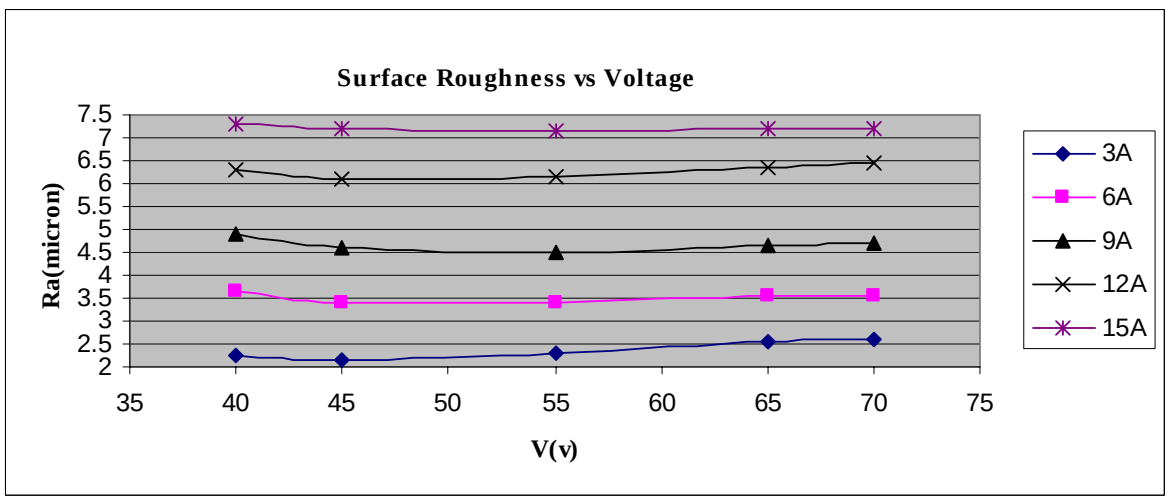

Fig. 16 Effect of source voltage on workpiece surface roughness.

In sum, the following items can also be mentioned as the general findings of the present research:

1- The BP and RBF neural networks are capable of constructing models using only experimental data, describing proper machining behavior. This is the main attraction of neural networks, which make them suitable for the problem at hand.

2- Modeling accuracy with neural networks is better than the common quadratic regression method. This is mainly due to the higher capabilities of ANNs in establishing data driven models, and also less sensitiv to noise in the experimental data.

3- RBF neural network which possesses the privileges of rapid learning, easy convergence and less error with respect to BP network, has better generalization power and is more accurate for this particular case. This selection was done according to the results obtained in the verification phase.

4- Discharge current is the dominant factor among other input parameters, so that, increasing current in a constant level of pulse period and source voltage,steadily increases MRR and Ra steadily.

A high discharge energy associated with high current is capable of removing a chunk of material leading to the formation of a deep and wide crater, and hence, worsening the machined surface quality.

5- For the effect of pulse period, initially, it is observed that for all values of source voltage and a constant current, material removal rate and surface roughness increase with increasing pulse period, but these trends continue until about 150 μsec of pulse period in which MRR gains its maximum value. Although, it is generally understood that increasing pulse period, and hence, pulse-on time, results in greater discharge energy, but with too long pulse durations, the results become reverse. This is mainly because of undesirable heat dissipation phenomena of the thermal energy liberated during discharge, which in turn lessens the erosive effects of sparks.

6- In normal EDM, the discharge voltage (V_{dis}), influenced primarily by the electrode and workpiece materials, is somehow constant so that an increase in source voltage will have little effect on the discharge energy for a given pair of electrode-workpiece materials. Hence, increasing source voltage alone, does not necessarily confirms the availability of high discharge voltage, which directly affects MRR and Ra.

7- High material removal rate and low surface roughness are conflicting goals, which cannot be achieved simultaneously with a particular combination of control setting. To achieve the optimum machining conditions, the goals have to be taken separately in different phases of work with different emphasis. In other words, three regimes of finishing, semi-finishing and roughing with relevant prescribed constraints on Ra need to be considered, and then optimization procedure (maximizing MRR) is done in each working domain.

This is the main issue of our future research which will be explained in a next paper.

10. References

[1] R. E. Williams, K. P. Rajurkar, "Study of wire electrical discharge machined surface characteristics", *J. Mater. Pro. Tech*, 28(1991), PP. 127-138.

[2] N. K. Jain, V. K. Jain, "Modeling of material removal in mechanical type advanced machining processes: a state-of-art review", *Int. J. Mach. Tools Manufact.*, 41(2001), PP. 1573-1635.

[3] S. M. Pandit, K. P. Rajurkar," *A* stochastic approach to thermal modeling applied to electro-discharge machining", Trans. *ASME J. Heat Transfer*, 105(1983), PP. 555-562.

[4] J. A. McGeough, *Advanced Methods of* Machining, Chapman and Hall, London and New York, 1988.

[5] F. Van Djick, Physico-mathematical analysis of the electro-discharge machining process, Ph.D. Thesis, Catholic University of Leuven, Belgium, 1973.

[6] A. Erden, B. kaftanoglu, "Heat transfer modeling of electric discharge machining", 21st MTDR Conference, Swansea, UK, Macmillan Press Ltd., 1980, PP. 351-358.

[7] S. T. Jilani, P. C. Pandey, "Analysis and modeling of EDM parameters", *Precision Engineering*, 4(4) (1982), PP. 215-221.

[8] A. Singh, A. Ghosh, "A thermo-electric model of material removal during electric discharge machining", *Int. J. Mach. Tools Manufact*., 39(1999), PP. 669-682.

[9] M. Ghoreishi, J. Atkinson, "Vibro-rotary electrode: a new technique in EDM drilling, performance evaluation by statistical modeling and optimization", *ISEM XIII*, Spain, May 2001, PP. 633-648.

[10] M. Ghoreishi, J. Atkinson, "A comparative experimental study of machining characteristics in vibratory, rotary and vibro-rotary electro-discharge machining", *J. Mater. Proc. Tech*., 120(2002), PP. 374-384.

[11] P. J. Wang, K. M. Tsai, Semi-empirical model on work removal and tool wear in electrical discharge machining, *J. Mater. Proc. Tech.*, 114(2001), PP. 1-17.

[12] K. M. Tsai, P. J. Wang, "Semi-empirical model of surface finish on electrical discharge machining", *Int. J. Mach. Tools Manufact*., 41(2001), PP. 1455-1477.

[13] J. A. Freeman, D. M. Skapura, *Neural Networks: algorithms, applications, and programming techniques*, Addision-Wesley, Reading. MA, 1992.

[14] J. Y. Kao, Y. S. Tarng, "A neural-network approach for the on-line monitoring of the electrical discharge machining process", *J. Mater. Proc. Tech*., 69(1997), PP. 112-119.

[15] H. S. Liu, Y. S. Tarng, "Monitoring of the electrical discharge machining process *by* abductive networks", *Int. J. Adv. Manufact. Tech.*, 13(1997), PP. 264-270.

[16] G. Indurkhya, K. P. Rajurkar, "Artificial neural network approach in modeling of EDM process", in: Proc. Artificial neural networks in engineering (ANNIE92) conf., st. Louis, Missouri, USA, 15-18 November 1992, PP. 845-850.

[17] T. A. Spedding, Z. Q. Wang, "Study on modeling of wire EDM process", *J. Mater. Proc. Tech.*, 69(1997), PP. 18-28.

[18] T. A. Spedding, Z. Q. Wang, "Parametric optimization and surface characterization of wire electrical discharge machining process", *Precision Engineering*, 20(1997), PP. 5-15.

[19] Y. S. Tarng, S. C. Ma, L. K. Chung, "Determination of optimal cutting parameters in wire electrical discharge machining", *Int. J. Mach. Tools Manufact.*, 35(1995), PP. 1693-1701.

[20] L. Fausett, *Fundamentals of neural networks: architectures, algorithms, and applications*, Prentice-Hall, Englewood Cliffs, NJ, 1994.

[21] D. R. Hush, B. G. Horne, "Progress in supervised neural networks", *IEEE Signal Processing Magazine*, January (1993), PP. 8-39.

[22] H. Demuth, M. Beale, *Neural Network Toolbox: for use with MATLAB*, user's guide, The Math Works, USA, 2000.

[23] K. Hornik, M. Stinchcombe, H. White, "Multilayer feed forward networks are universal approximators", Neural networks, 2(1989), PP. 359-366.

[24] C. M. Bishop, *Neural networks for pattern recognition*, Oxford: Oxford University Press, 1995, P. 372.

[25] D. C. Montgomery, E. A. Peck, *Introduction to linear regression analysis*, Wiley, New York, 1992.

[26] S. Assarzadeh, Modeling of material removal rate and surface roughness in Electro-Discharge Machining (EDM) process using artificial neural networks (ANNs), M.S. Thesis, Department of Mechanical Engineering, K.N. Toosi University of Technology, Tehran, Iran, 2003.